EUROPEAN ORGANIZATION FOR NUCLEAR RESEARCH
CERN - ACCELERATORS AND TECHNOLOGY SECTOR

CERN-ATS-2012-019

Performance of a Fast Digital Integrator in on-field Magnetic Measurements for Particle Accelerators

P. Arpaia,[1] L. Bottura,[2] L Fiscarelli,[1,2] and L. Walckiers[2]
1 Department of Engineering, University of Sannio, Benevento, Italy
2 CERN, Geneva, Switzerland

Abstract

The fast digital integrator has been conceived to face most demanding magnet test requirements with a resolution of 10 ppm, a signal-to-noise ratio of 105 dB at 20 kHz, a time resolution of 50 ns, an offset of 10 ppm, and on-line processing. In this paper, the on-field achievements of the fast digital integrator are assessed by a specific measurement campaign at the European Organization for Nuclear Research (CERN). At first, the architecture and the metrological specifications of the instrument are reported. Then, the recent on-field achievements of (i) ±10 ppm of uncertainty in the measurement of the main field for superconducting magnets characterization, (ii) ±0.02% of field uncertainty in quality assessment of small-aperture permanent magnets, and (iii) ±0.15% of drift, in an excitation current measurement of 600 s under cryogenic conditions, are presented and discussed.

Published in Review of Scientific Instruments (2012)

Geneva, Switzerland

February 2012

Performance of a fast digital integrator in on-field magnetic measurements for particle accelerators

P. Arpaia,[1] L. Bottura,[2] L. Fiscarelli,[1,2] and L. Walckiers[2]
[1]*Engineering Department, University of Sannio, 82100 Benevento, Italy*
[2]*European Organization for Nuclear Research (CERN), 1217 Geneva, Switzerland*

(Received 6 June 2011; accepted 5 December 2011; published online 2 February 2012)

The fast digital integrator has been conceived to face most demanding magnet test requirements with a resolution of 10 ppm, a signal-to-noise ratio of 105 dB at 20 kHz, a time resolution of 50 ns, an offset of 10 ppm, and on-line processing. In this paper, the on-field achievements of the fast digital integrator are assessed by a specific measurement campaign at the European Organization for Nuclear Research (CERN). At first, the architecture and the metrological specifications of the instrument are reported. Then, the recent on-field achievements of (i) ±10 ppm of uncertainty in the measurement of the main field for superconducting magnets characterization, (ii) ±0.02 % of field uncertainty in quality assessment of small-aperture permanent magnets, and (iii) ±0.15 % of drift, in an excitation current measurement of 600 s under cryogenic conditions, are presented and discussed.
 [doi:10.1063/1.3673000]

I. INTRODUCTION

The most relevant specifications of the magnetic field produced by accelerator magnets are strength and direction, errors with respect to the ideal profile, and location of the magnetic axis (in the case of quadrupole magnets giving field gradients).[1] The above quantities are required as integral or average over the magnet length. Ideally, the selection of the measurement instrument should be based on the field range to be measured, the required accuracy, the mapped volume, and the frequency bandwidth.

The range of field to be measured across particle accelerator magnets is large, spanning several orders of magnitude, from fields as low as 0.1 mT (corrector magnets in warm conditions) to peak fields of the order of 10 T (main bending superconducting dipoles at ultimate field). For the accuracy, the production follow-up and the accelerator operation requires knowledge of the magnetic field better than 100 ppm or, as often referred to in relative terms, 1 unit, i.e., 10^{-4} of the main field.[1] Traditionally, at this accuracy level, these quantities are measured by means of rotating coils.[2–4] For specific tasks, such as quadrupole gradient and axis measurements, or for fast sextupole component measurements, other techniques, such as single stretched wire,[5] or Hall probe arrangements, are applied.[6] In practice, only fluxmeter methods (stationary or rotating coils read by voltage integrators) and magnetic resonance devices (NMR/EPR) can satisfy the requirements of 100 ppm accuracy over a range of 10 T, while Hall probes are only marginally applicable.[7–9]

An advantage of fluxmeters is that the sensing device, the coil itself, can be made perfectly linear, by using only non-conducting and non-magnetic components (ceramics and plastics) and by decreasing the calibration burden significantly. Magnetic resonance probes, as well as Hall probes, have local nature and are not suited to the effective measurement of integral field over length of several meters. This is possible by using assemblies of coils used as probes in a rotating-coil or fixed-coil fluxmeter. This is why many magnetic measurement techniques, from magnetic diagnostic in tokamak[10–13] to high-current superconducting-cable test,[14] rely on the use of an integrator. In field measurements for accelerator magnets, the integrator requirements are imposed mainly by the most-demanding measurement objectives of rotating coils.

Altogether, a maximum rotation speed of 10 turns/s and a maximum angular resolution of 8192 points per turn give rise to a flux sampling rate of about 150 kS/s as a target. Typical requirements[15] (for a full-scale input signal of ±10 V) are a SNR higher than 80 dB, at a sampling rate of 150 kS/s, a ±10 ppm target for the non-linearity, and ±10 ppm target for 1-h stability of gain and offset (Table I).

These requirements are not met by the Portable Digital Integrator (PDI),[16] in use for over 20 years. In fact, the PDI, based on a voltage-to-frequency converter (VFC) with a maximum frequency of 500 kHz and a full scale of 10 V, has a resolution of 2×10^{-5} Vs for a gain of 1. This value is associated with the uncertainty on the increment flux due to the rounding of the counter. The relative uncertainty on the flux increment depends not only on the amplitude of the input signal but also on the measurement time interval. In fact, for a VFC, a larger measurement time gives higher accuracy. Therefore, the accuracy of a VFC gets worse on increasing the sampling rate, not satisfying the above requirements of fast magnetic transducers.[17,18]

At this aim, several new integrators were conceived (at "Commisariat à l'Energie Atomique" of CEA Saclay,[19]

TABLE I. Fast rotating coil requirements.

Rotation speed (turns/s)	10
Angular resolution (rad)	10^{-3}
Flux sampling rate (kS/s)	150
SNR (dB)	80
Linearity error (ppm)	±10
1-hour stability (ppm)	±10

at the Japan Atomic Energy Research Institute,[20] and at the Fermi National Accelerator Laboratory[21]), but without making available an instrument for a direct on-field exploitation. A new fully on-board instrument, the Fast Digital Integrator (FDI), was developed at the European Organization for Nuclear Research (CERN), in cooperation with the University of Sannio.[22] A metrological characterization, both in simulation[23,24] and in laboratory,[15,25] was carried out, by highlighting frequency bandwidth and accuracy significantly higher than the de-facto standard PDI.

In this paper, the on-field performance evaluation of the fast digital integrator, promising new performance to magnetic measurements for particle accelerators, is reported. The performance achievement of the instrument, such as magnetic field precision and integration drift, in three high-demanding applications, such as superconducting magnet analysis, small-aperture permanent magnets characterization, and superconducting cables testing, are illustrated and discussed. In particular, in Sec. II, the architecture and the metrological specifications of the fast digital integrator are highlighted. In Sec. III, the on-field achievements of the instrument in the analysis of dynamic errors of superconducting magnets are presented. In Sec. IV, the results in characterizing small-aperture permanent magnets are illustrated. Finally in Sec. V, the drift performance in the measurement of currents at cryogenic temperature is analyzed.

II. FAST DIGITAL INTEGRATOR

In the following, (A) the *architecture* and (B) the *metrological specifications* of the fast digital integrator are recalled.

A. Architecture

The input signal is conditioned by a differential gain amplifier (PGA in Fig. 1), with self-calibration capabilities, and sampled in the time domain by a high-speed, high-resolution successive approximation register (SAR) ADC (Table II). A DSP is the numerical core of the board, processing measurement data and supervising the board as a whole, in association with a field programmable gate array (FPGA). In particular, the FPGA provides the DSP with a powerful I/O capability,

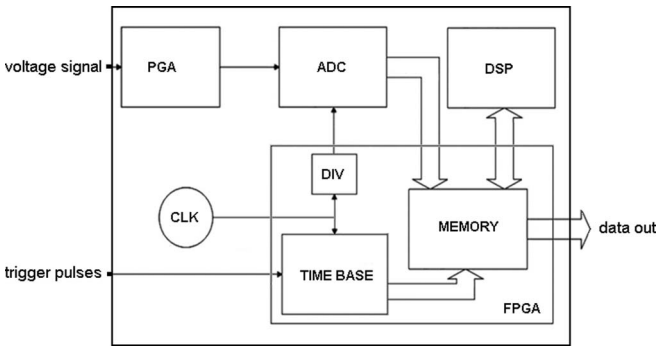

FIG. 1. FDI conceptual architecture (PGA: programmable gain amplifier, CLK: clock, ADC: analog-to-digital converter, DIV: divider, DSP: digital signal processor, FPGA: field programmable gate array).

TABLE II. SAR ADC specifications.

Resolution (bit)	18
Max sampling rate (kS/s)	670
Integral linearity error (LSB)	±1.5
Bipolar zero error (%FS)	±0.03
Zero error temperature drift (ppm/°C)	±0.5
Bipolar full-scale error (%FS)	±0.09
Full-scale error temperature drift (ppm/°C)	±0.5

by acting as interface for the DSP with the local bus and with the memory (Fig. 1).

With respect to a last-generation digital signal controllers,[26] this simultaneous presence of DSP and FPGA allows both state-of-the-art maximum processing power and large I/O capabilities. The DSP carries out the numerical integration, by releasing a magnetic flux sample at each trigger pulse. Trapezoidal rule was selected as integration algorithm by means of a suitable uncertainty computational overhead analysis.[24] Thus, the trigger frequency represents the flux sampling rate, with a theoretical maximum value limited by the ADC Nyquist frequency. The maximum sampling rate of the ADC of FDI is 500 kS/s in order to have an integer ratio with the main clock frequency. Therefore, the instrument can accept a maximum trigger rate of the half ADC rate (at least two ADC samples for each defined integral), and thus is capable of analyzing the flux over a bandwidth of 125 kHz.

The main advantages of on-board processing are: (i) to deal with the asynchronous trigger signal from angular encoders coupled with rotating shafts without losing performance, and (ii) to reduce the data flow and memory demand to the controlling PC. In particular, the DSP processes generic algorithms like on-line integration.[25] On-line integration means that each flux sample is processed inside one sampling period by allowing dynamic performance and throughput to be maintained, so as to attain the desired speed in the *fast* digital integrator.

A further uncertainty reduction of the measured integral values is achieved by exploiting a universal time counter (UTC), with resolution of 50 ns, used to measure the absolute time of the external trigger signal, asynchronous with respect to the ADC conversion signal (ADC clock). At this aim, a 20-MHz oven-controlled crystal oscillator, with phase noise of –140 dBc/Hz at 1 kHz and ±0.3 ppm of long-term stability (1 year), is used as time base for the UTC. The oscillator loads a 40-bit counter implemented on the FPGA, by providing an accurate time measurement on a time up to 15 h.

The integration algorithm is based on the trapezoidal rule. The first trigger pulse enables the UTC. Then, at each ADC sample, the area of a trapezoidal element (Fig. 2) is computed, by knowing the last ADC sample and the period τ_c, and accumulated. The step is repeated until a second trigger pulse arrives. The assessment of the time intervals τ_a (time between a trigger pulse and the next ADC sample) and τ_b (time between the last ADC sample and the trigger pulse), depicted in Fig. 2, is crucial in order to reduce the numerical integration

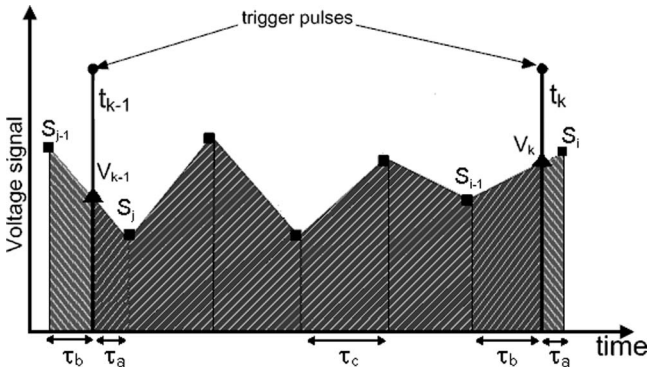

FIG. 2. Integration algorithm: V_k (▲) are computed by means of a linear interpolation between the previous S_{i-1} and the next S_i ADC sample (■).τ_a and τ_{ba} are known by the on board UTC.

error. They are measured by means of the UTC and the voltage V_k is obtained by a linear interpolation of the previous (S_{i-1}) and the next (S_i) ADC sample with respect to arrival time t_k of the trigger pulse.[24]

B. Metrological specifications

Typical static non-linearity, relative to a full scale of ±10 Vs and with temperature ranging between 27 and 35 °C, is within ±7 ppm.[27] The transfer function has typical gain relative errors of 0.2% with respect to its nominal value 1 and typical offset errors of 17 ppm relative to the full scale.

Typical repeatability value is ±1 ppm over 30 min at 30 °C, when electromagnetic noise is minimized by extracting the board out of the PXI crate.

Typical values of 24-h stability are about ±3 ppm. Furthermore, the transfer function, extrapolated on the basis of the stability test, provides an estimation of the relative 24-h stability for the FDI gain and offset.

In Fig. 3, theoretical and typical dynamic performance of FDI and PDI, expressed as signal-to-noise and distortion ratio (SINAD) (Ref. 29) of the integrated signal as a function of the trigger frequency, are compared.[28] The acquisitions were performed in nominal conditions of coherent sampling, by synchronizing the trigger signal with the board clock, and the actual spectral leakage was attenuated by using a Blackman-Harris window.[25] The comparison shows a remarkable improvement achieved by the FDI by about 40 dB in comparison to the PDI. Moreover, its performance is evaluated also in working conditions not accessible to PDI. In the above bandwidth, the SINAD is higher than 100 dB, namely, the required target of 10 ppm is achieved.

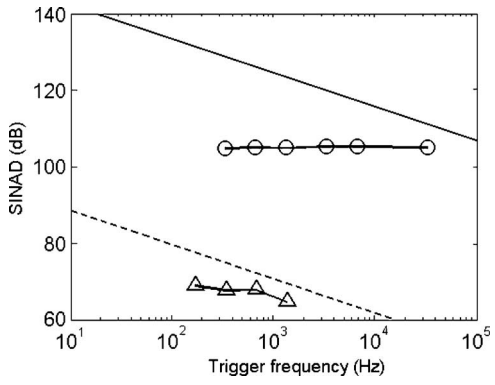

FIG. 3. FDI (o) and PDI (Δ) dynamic performance vs. trigger frequency, for an input sine wave of 10 Hz and 10 V peak to peak, measured for 2 s.[25] The theoretical performance limit is reported with a dotted line for PDI and a solid line for FDI.

III. TESTING DYNAMIC ERRORS OF SUPERCONDUCTING MAGNETS

Acceleration operation of a collider requires constant magnetic field phases for particles injection. The acceleration cycle of the Large Hadron Collider (LHC) at CERN includes a constant current plateau in the dipoles of about 760 A for more than 1000 s (Fig. 4). Previous experiences with superconducting magnet collider (HERA, TEVATRON, and SSC) highlighted that, during contant current phases, the magnetic field components inside the superconducting magnets change by showing a "decay" effect.[29] The field change can be also large if compared to the tolerances of the accelerator machine (about 20 units of chromaticity) and needs to be corrected accurately. The dependency of the powering history of this phenomenon requires a parametric study based on measurement campaigns and feedbacks from operations.

At the end of the injection plateau, as soon as the magnet current is increased, all the field harmonics go back to the initial values at the beginning of the plateau. This fast effect is called "snapback."[30] If not compensated suitably, the corresponding sudden variation of magnetic field components, mainly of the sextupole (b_3) and decapole (b_5) multipoles, affect deeply the beam dynamic properties.

During the construction phase of the LHC dipole series, the amplitude of the decay was measured by using the PDI.[16] A 15-m long shaft, composed of 12 ceramic segments[17] and equipped by coil-based transducers, was turning inside the magnet aperture. The coil signals were integrated in the time domain between fixed angular positions, time stamped by an angular encoder in order to get the magnetic flux. The flux sampling rate depends on the angular speed and on the number of points per turn. The multipolar components of the magnet under test are evaluated for each turn of the coil, thus a faster rotation gives a higher update rate of field harmonics. The time resolution of 20 s given by the old PDI-based acquisition system was not sufficient to measure the snapback

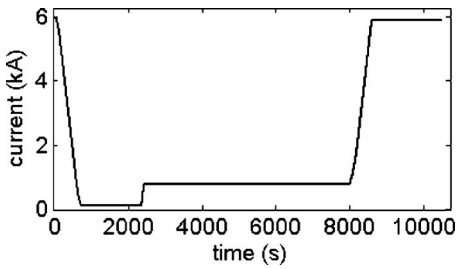

FIG. 4. Example of a present LHC current cycle: preparation plateau at 100 A, injection plateau at 757 A for 5500 s, parabolic-exponential-linear acceleration ramp, and physics plateau at 5890 A.

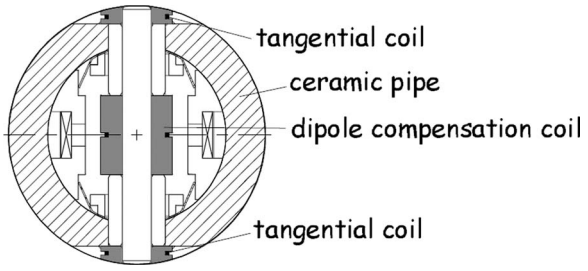

FIG. 5. Details of support and coils in the cross-section of a segment.[17]

occurring in some seconds at the current ramp start. This was done on a limited number of magnets using a system based on Hall plates. The FDI, as well as a new generation of motor/encoder units,[31] were developed in order to measure the magnetic field with higher bandwidth.

The new configuration is based on 12 FDI boards. Two sets of three boards are used to measure the main dipole components separately on the ends and on the central parts of each dipole aperture. This main field component is measured by the central coil sketched in the shaft cross-section of Fig. 5. Six other FDI integrators measure the higher harmonic components, by connecting a tangential and the central coils in opposition in order to cancel the main component and enhance the signal-to-noise ratio. The measuring shafts are rotated up to 10 turns/s by a motor unit including angular encoder and slip rings for the coil signals (Fig. 6). The magnetic flux is measured between 512 angular positions per turns, thus each integrator produces more than 5'000 integrated voltage samples per second.

In Figs. 7, the behavior of the magnet transfer function (TF, namely, the ratio of the main field to the current, Fig. 7(a)) and the more critical magnetic field components b_3, b_5, and b_7 (Figs. 7(b)–7(d), respectively) are shown. They are measured during the injection plateau (1000 s at 760 A) and the initial acceleration ramp. They are expressed as variation from the starting value (t = 0), and depicted as integral value, over the total shaft length, at the reference radius of 17 mm. The precision of the multipolar components (Figs. 7(b)–7(d) is higher than the transfer function (Fig. 7(a)), because (i) a suitable bucking of the main harmonic is realized by connecting in anti-series the central and the tangential coils, and (ii) the multipolar components are referred to the main field measured by the central coil.

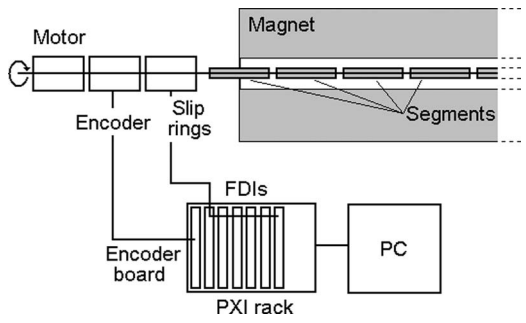

FIG. 6. Rotating coil measurement system for LHC main dipole testing.

In particular, the decay (for time < 1000 s) and the snapback (for time > 1000 s) can be recognized easily. For the transfer function (Fig. 7(a)), evaluated by analyzing the absolute signal of the central coil, a 1-σ uncertainty band of ± 10 ppm allows a decay of about 60 ppm and a snapback of about 150 ppm to be assessed. Such a band corresponds to a SNR of more than 90 dB, not reachable by means of the PDI. The time resolution of 1 s for all the measured field components allows the fast dynamic errors to be studied and investigated suitably. Furthermore, this study case highlights the usefulness of the on-board integration algorithm: besides the higher accuracy, the size of the transferred and stored flux data is reduced by a factor in the order of 500.

Finally, the new FDI-based measurement system, after several measurement campaigns aimed at validating the LHC magnetic model, allows both multipoles to be measured with very-high precision and field errors to be corrected with residuals in the order of few ppm.[32]

IV. TESTING SMALL-APERTURE MAGNETS

Presently, a new linear accelerator Linac4 for the injection of ions H^- with target energy of 160 MeV is under construction at CERN.[33] For one of its main sections, the first drift tube tank, a set of permanent magnet quadrupoles (PMQ) are employed for focusing the beam. They were selected as the best practical way to provide the required high gradient within the small volume available inside the high-frequency accelerating structure. Additional advantages include simple fixed-optics operation and no need of cooling. The PMQs are tuned in focusing-defocusing pairs with the same integrated gradient. The tuning of the gradient is done by the magnet manufacturer and is verified at CERN, according to a common measurement reference, as a part of the acceptance tests of each magnet. Their main parameters are reported in Table III. The drift tubes are not adjustable in any way, thus corrective interventions on assembled tanks would be very costly and must absolutely be avoided.

Testing magnets as the PMQs with a small aperture of the order or 20 mm is a challenging task. The requirements for the field quality assessment of such magnets are in the order of units (10^{-4} of the main field). In general, small coil shafts suffer from the non-negligible physical dimensions of the winding. The machining defects became determinant in the overall uncertainty of the rotating coil. Furthermore, the shaft speed must be high (1 turn/s) in order to increase the SNR despite the low sensitivity coefficient (surface) of the coil.

TABLE III. Permanent magnet quadrupoles main parameters.

Parameter	Value
Peak gradient (T/m)	23.6–58.4
Integrated gradient (Tm/m)	1.0–2.5
Length (mm)	45–80
Bore diameter (mm)	22
Reference radius R_{ref} (mm)	7.5
Outer diameter (mm)	60

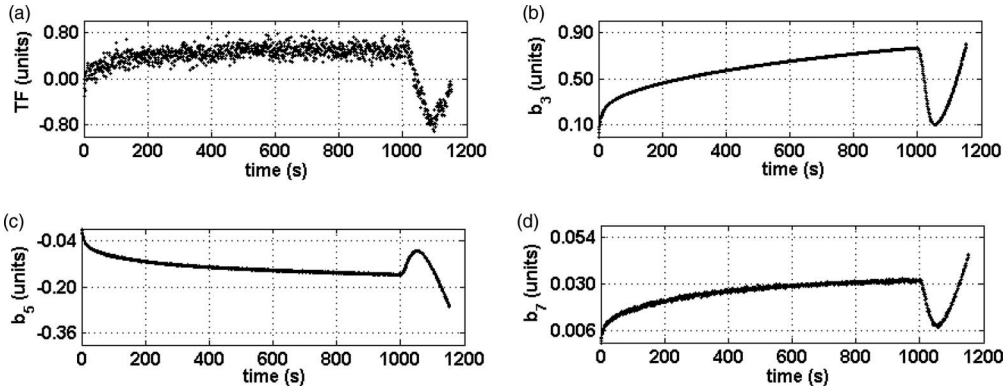

FIG. 7. Measurement results of the variations from the initial value (t = 0) for: (a) magnet transfer function TF, (b) sextupolar component b_3, (c) decapolar component b_5, and (d) 14-pole component b_7, measured at the reference radius of 17 mm during injection plateau and initial acceleration ramp.

The measurement station for the PMQs is based on a rotating coil system developed at CERN (Fig. 8). The bench is equipped with: (i) a motor unit, (ii) a coil shaft with length 200 mm and diameter of 19 mm, (iii) an encoder unit mounted on the shaft on the opposite side of the motor, (iv) a PXI encoder board to manage the angular trigger signal (2048 points per turn), and (v) a fast digital integrator to acquire and process the signal from the coil.

In this case, the field quality of the magnets was assessed in terms of multipolar coefficients by analyzing the signal of a single coil.

Preliminarily, deterministic errors were corrected by taking the difference of several measurements with the magnet in different positions ("rotation and reflection of axis"[34]). Then, the relative uncertainty of Type A was computed for each multipolar coefficient. As a further verification, the measured multipoles were compared to the measurements made by the factory and differences less than 2 units in average were observed. The resulting uncertainty, up to the 10th coefficient, is summarized in Table IV: the FDI allows the target of ±0.02 % of uncertainty in field quality assessment to be reached, owing to its negligible noise contribution. The PDI cannot be used for the same measurement: its SINAD less than 70 dB (Fig. 3) affects the results significantly, by introducing an amount of uncertainty well above the other sources (such as mechanical defects).

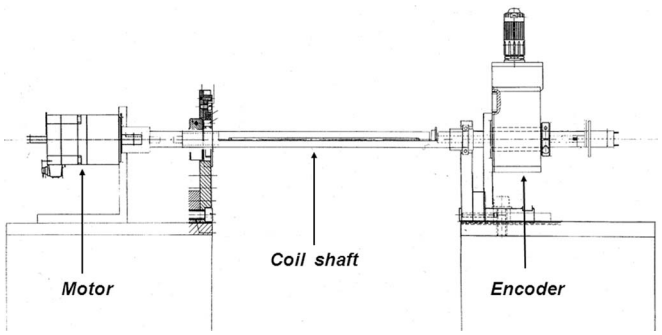

FIG. 8. Rotating coil measurement bench for the Linac4 permanent quadrupole.

V. CURRENT MEASUREMENTS AT CRYOGENIC TEMPERATURE

Testing superconducting cables is another field for which a fast and precise integration is useful.[14] Usually, the evaluation of critical currents requires injecting and measuring currents in the cable sample in the order of several tens of kA, with a variable magnetic field background and by preserving the cryogenic conditions. This is done commonly by means of high-current power supplies requiring equal capacity feed through. The electro-mechanical set-up has very large dimensions, and leads to large demands to the cryogenic plant. An alternative is to use a superconducting transformer. It is composed by (i) two air-cored coils, usually called "primary" winding, directly fed by the power supply and producing a variable magnetic field, and (ii) a "secondary" winding, where the current is induced by the field variation. A secondary-current measurement device and a feedback control system are needed to drive the feeding of the primary, in order to have the desired current profile as output. Currents have to be measured at low temperature because the secondary of the transformer is connected to the cable under test directly into the cryostat. Most of the standard methods are not suitable for large currents in cryogenic conditions, and only simpler techniques can be applied directly. Rogowski coils and integrators are a trade-off between application ease and measurement quality.[35] Their main drawback arises from unavoidable drifts in long measurements.

At the Facility for the Research on Superconducting Cables (FReSCa) of CERN,[36] the cable test station has been

TABLE IV. Multipolar component uncertainty.

Multipole order	Average value (units)	Relative uncertainty (units)
c_3	24.4	1.3
c_4	49.1	1.5
c_5	11.8	1.7
c_6	20.6	0.7
c_7	7.0	2.3
c_8	1.5	2.5
c_9	0.7	1.2
c_{10}	1.1	0.8

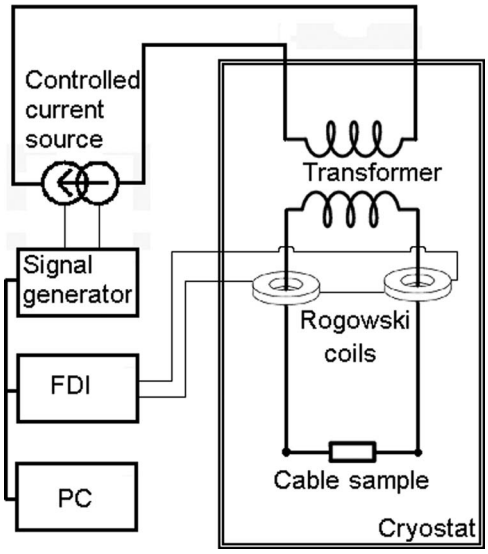

FIG. 9. Schematic of the cryo-transformer and its current measurement and control system.

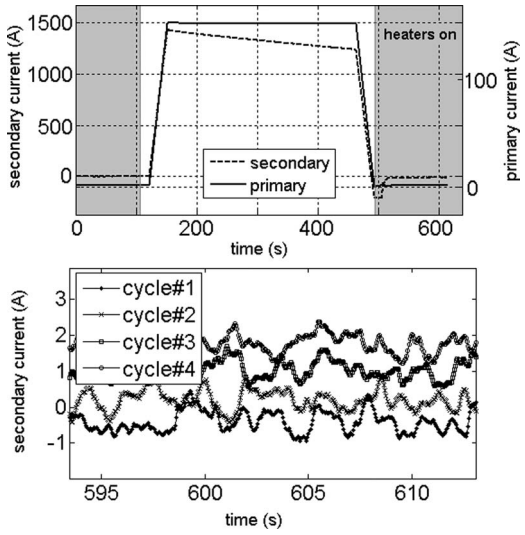

FIG. 10. Open-loop current cycles measured on the transformer secondary and primary to assess the drift: (a) the whole cycles and (b) a detail of the drift on the secondary current at the end of several cycles (heaters' switched-on times highlighted in gray).

upgraded by introducing a cryo-transformer developed a few years ago and newly equipped with a fully digital control system, based on the fast digital integrator, and relying on its high resolution and stability. The current circulating in the secondary of the transformer and in the sample is measured by means of two toroidal Rogowski coils (Table V). They are placed around the two output cables of the secondary (Fig. 9), above the connection area. Each coil consists of about 2600 turns of 0.1-mm copper wire.

Theoretically, a perfectly wound Rogowski coil is insensitive to external magnetic field variations. However, owing to winding inaccuracy, perturbations arising from the field generated by the transformer can be detected. The external field influence is minimized, by increasing also the signal simultaneously, by connecting the two coils in an anti-series compensation scheme.

The signal is acquired by a fast digital integrator, with a trigger signal of 20 Hz provided by a PXI timing board. However, the coils allow only the current variations to be measured, thus the initial value of the current has to be known when the integration is started. To this aim, a null secondary current is obtained by means of suitable heaters, mounted on the secondary to warm up the cable above the critical temperature.

The measurement system as a whole was characterized by assessing its resolution and drift. The resolution was estimated by analyzing the signal-to-noise ratio (SNR) during a high-current plateau. For a current of 10 kA, the SNR resulted higher than 80 dB, by leading to a resolution of the current less than 1 A. The drift was assessed as the variation in the measured current between the initial and the final values of a powering closed-cycle of long duration. In Fig. 10(a), examples of current measurements in a long-duration test of about 600 s are shown. Open-loop cycles (without activating the feedback control system) composed by two ascending/descending ramps from 0 to 150 A on the primary, were performed. The secondary was connected to a superconducting short circuit (a piece of standard LHC Rutherford cable) and was excited by a current up to 1.4 kA. At the end of the cycles, the heaters were switched on, in order to force the zero current by warming up the secondary and making it resistive. The final measured current is in the range of ± 2 A (± 0.15 %), corresponding to a time average drift of ± 3.3 mA/s (Fig. 10(b)). This drift corresponds to less than 1 ppm in term of voltage offset and is compatible with the FDI stability specifications (7 ppm in 24 h). Such a drift meets the requirement target of uncertainty in current estimation for superconducting cable tests of thousands seconds and overcomes by a factor 30 the performance (0.1 A/s of drift) of the previous system[37] based on custom electronics.

TABLE V. Rogowski coil main parameters.

Parameter	Coil 1	Coil 2
R_{int} (mm)	26	26
R_{ext} (mm)	57	57
Width (mm)	72.1	72.1
Number of turns	2615	2569

VI. CONCLUSIONS

The fast digital integrator , based on a high-rate 18-bit resolution analog-to-digital converter and a digital signal processor , has been tested and validated on the field at CERN. The FDI overcomes the limits in terms of frequency bandwidth and accuracy of the de-facto standard integrator, the portable digital integrator, previously used at CERN, as well as in many other research centers. The instrument has been exploited in several challenging measurements in the magnetic area, such as dynamic field error characterization in superconducting magnets, small-aperture magnet quality assessment, and current measurement in cryogenic conditions.

For superconducting magnets, a 1-σ uncertainty band of $\pm$ 10 ppm for the transfer function (field divided by excitation current) is measured. The time variation of the "decay" and "snapback" of the sextupole component is measured with unprecedented precision, allowing a correction in the order of few ppm.[32] Furthermore, owing to the on-board integration algorithm, besides the higher accuracy, the size of the transferred and stored flux data is reduced by a factor in the order of 500. For small-aperture magnets, the FDI allows the target of $\pm$0.02% of field uncertainty to be reached owing to its negligible noise contribution with respect to PDI. For cryogenic current measurements, the FDI stability produces a drift of $\pm$0.15% in 600 s, meeting the uncertainty target and overcoming by a factor 30 the performance of the previous system.

The use of the instrument at CERN as well as in other laboratories allowed the refinement of the instrument, by launching the FDI to become the new de-facto standard integrator for magnetic measurements.

ACKNOWLEDGMENTS

This work was supported by CERN trough the agreement KE1776/TE with the University of Sannio, whose support authors acknowledge gratefully. The authors thank M. Buzio, B. Celano, F. Cennamo, P. Cimmino, C. Giaccio, D. Giloteaux, G. Golluccio, V. Inglese, A. Masi, G. Montenero, J. G. Perez, and G. Spiezia for their useful suggestions and cooperation.

[1] A. Chao and M. Tigner, *Handbook of Accelerator Physics and Engineering*, 2nd ed. (World Scientific Publishing, London, 1999).
[2] L. Walckiers, "Magnetic measurement with coils and wires," in *CERN Accelerator School CAS 2009: Specialised Course on Magnets, Bruges, 16–25 June 2009* (CERN, Bruges, 2009), pp. 357–385, http://arxiv.org/abs/1104.3784v1.
[3] G. Sinha and G. Singh, Rev. Sci. Instrum. **79**, 123302 (2008).
[4] J. Fujita, K. Matsuura, K. Kawahata, S. Fujiwaka, S. Itoh, K. N. Sato, K. Nakamura, H. Zushi, M. Sakamoto, K. Hanada, E. Jotaki, and K. Makino, Rev. Sci. Instrum. **70**(1), 445 (1999).
[5] J. DiMarco and J. Krzywinski, MTF single stretched wire system, Technical Report MTF-96-0001, Fermi National Accelerator Laboratory, 1996.
[6] L. Bottura, L. Larsson, S. Schloss, M. Schneider, N. Smirnov, and M. Haverkamp, IEEE Trans. Appl. Supercond. **10**(1), 1435 (2000).
[7] C. Schott, R. S. Popovic, S. Alberti, and M. Q. Tranb, Rev. Sci. Instrum. **70**(6), 2703 (1999).
[8] K. N. Henrichsen, "Classification of magnetic measurement methods," in *CERN Accelerator School, Magnetic Measurement and Alignment*, Montreux, 16–20 March 1992 (CERN, Montreux, 1992), pp. 70–83, http://cdsweb.cern.ch/record/245401/files/p70.pdf.
[9] L. Bottura and K. Henrichsen, "Field measurements," in *CERN Accelerator School, Superconductivity and Cryogenics for Particle Accelerators and Detectors*, Erice, 8–17 May 2002 (CERN, Erice, 2002), pp. 118–148, http://cdsweb.cern.ch/record/592467/files/lhc-2002-011.pdf.
[10] J. G. Bak, S. G. Lee, D. Son, and E. M. Ga, Rev. Sci. Instrum. **78**, 043504 (2007).
[11] Seong-Heon Seo, A. Werner, and M. Marquardt, Rev. Sci. Instrum. **81**, 123507 (2010).
[12] D. M. Liu, B. N. Wan, Y. Wang, Y. C. Wu, B. Shen, Z. S. Ji, and J. R. Luo, Rev. Sci. Instrum. **80**, 053506 (2009).
[13] S. Holt and P. Skyba, Rev. Sci. Instrum. **78**, 036109 (2007).
[14] A. Godeke, D. R. Dietderich, J. M. Joseph, J. Lizarazo, S. O. Prestemon, G. Miller, and H. W. Weijers, Rev. Sci. Instrum. **81**, 035107 (2010).
[15] G. Spiezia, Ph.D. dissertation Univeristy of Naples FEDERICO II and CERN AT/MTM, 2008.
[16] P. Galbraith, Portable Digital Integrator, CERN Internal Technical Note 93-50, AT-MA/PF/fm January 1993, http://cdsweb.cern.ch/record/1362025/files/Portable_Digital_Integrator_1993.pdf.
[17] J. Billan, L. Bottura, M. Buzio, G. D'Angelo, G. Deferne, O. Dunkel, P. Legrand, A. Rijllart, A. Siemko, P. Sievers, S. Schloss, and L. Walckiers, IEEE Trans. Appl. Supercond. **10**(1), 1422 (2000).
[18] M. Haverkamp, L. Bottura, E. Benedico, S. Sanfilippo, B. ten Haken, and H. H. J. ten Kate, IEEE Trans. Appl. Supercond. **12**(1), 86 (2002).
[19] C. Evesque, in *Proceedings of International Magnetic Measurement Workshop IMMW11*, Upton, 21–24 September 1999 (Brookhaven National Laboratory, Upton, 1999).
[20] Y. Kawamata, I. Yonekawa, and K. Kurihara, *19th Symposium On Fusion Engineering*, Atlantic City, 22–25 January 2002 (IEEE/NPSS, Atlantic City, 2002) pp. 172–175, (2002).
[21] G. V. Velev, R. Carcagno, J. DiMarco, S. Kotelnikov, M. Lamm, A. Makulski, V. Maroussov, R. Nehring, J. Nogiec, D. Orris, O. Poukhov, F. Prakoshyn, P. Schlabach, and J. C. Tompkins, IEEE Trans. Appl. Supercond. **16**(2), 1374 (2006).
[22] P. Arpaia, A. Masi, and G. Spiezia, IEEE Trans. Instrum. Meas. **56**(2), 216 (2007).
[23] P. Arpaia, V. Inglese, G. Spiezia, and S. Tiso, IEEE Trans. Instrum. Meas. **58**(7), 1919 (2009).
[24] P. Arpaia, L. Bottura, A. Masi, and G. Spiezia, Meas. J. **41**, 737 (2008).
[25] P. Arpaia, V. Inglese, and G. Spiezia, IEEE Trans. Instrum. Meas. **58**(7), 2132 (2009).
[26] See http://www.analog.com/en/processors-dsp/sharc/adsp-21262/processors/product.html for ADSP-21262 Data Sheet, 2011.
[27] ISO ENV 13005. "Guide to the expression of uncertainty in measurement," Geneva, 1995.
[28] IEEE std 1057-1994. IEEE Standard for Digitizing Waveform Recorders, 1994.
[29] O. Brüning, LHC Project Note 218, February 2000.
[30] L. Bottura, "Field dynamics in superconducting magnets for particle accelerators," in *CERN Accelerator School on Measurement and Alignment of Accelerator and Detector Magnets*, Anacapri, 11–17 April 1997 (CERN, Anacapri, 1997) pp. 79–106, http://cdsweb.cern.ch/record/382436/files/p79.pdf.
[31] N. R. Brooks, L. Bottura, J. G. Perez, O. Dunkel, and L. Walckiers, IEEE Trans. Appl. Supercond. **18**(2), 1617 (2008).
[32] P. Arpaia, L. Fiscarelli, G. Montenero and L. Walckiers, Nucl. Instrum. Methods Phys. Res. A **638**(1), 176 (2011).
[33] F. Gerigk and M. Vretenar, Linac4 Technical Design Report CERN.AB.2006.084, December 2006.
[34] A. K. Jain, "Basic theory of magnets," in *CERN Accelerator School on Measurement and Alignment of Accelerator and Detector Magnets*, Anacapri, 11–17 April 1997 (CERN, Anacapri, 1997) pp. 1–26, http://cdsweb.cern.ch/record/1246515/files/p1.pdf.
[35] W. F. Ray, in IEE Colloquium on Low Frequency Power Measurement and Analysis, London, 2 November 1994, No. 203, pp. 1–6, (1994).
[36] A. P. Verweij and A. K. Ghosh, IEEE Trans. Appl. Supercond. **17**(2), 1454 (2007).
[37] A. P. Verweij, C.-H. Denarie, S. Geminian, and O. Vincent-Viry, IOP J. Phys. Conf. Ser. **43**, 833 (2006).